Available online at www.sciencedirect.com
SCIENCE DIRECT®

Geomorphology 75 (2006) 437–449

GEOMORPHOLOGY

www.elsevier.com/locate/geomorph

# Investigating the spatial distribution of summit flats in the Uinta Mountains of northeastern Utah, USA

Jeffrey S. Munroe

*Geology Department, Middlebury College, Middlebury, VT 05753, USA*

Received 29 November 2004; accepted 27 July 2005
Available online 15 November 2005

**Abstract**

Isolated, laterally extensive, gently sloping surfaces known as summit flats are present at high elevations in many Laramide ranges, and are particularly well developed in the Uinta Mountains of northeastern Utah. To investigate the spatial distribution of these surfaces, and to consider possible controls on this pattern, a map of summit flats in the Uintas was developed from digital elevation data. Summit flats were identified as unglaciated areas of the landscape above an elevation of 3400 m, having a slope of less than 0.3 m $m^{-1}$, and an area greater than $5 \times 10^{-2}$ $km^2$. As defined, summit flats comprise 43% of the unglaciated land area above 3400 m in the Uintas, with the largest individual flat covering nearly 34 $km^2$. To quantitatively evaluate the distribution of summit flats in the Uintas, the area of summit flats was normalized to the total unglaciated area above 3400 m in 10-km-wide swaths oriented normal to the range axis. Values of percent summit flats obtained by this method decrease dramatically westward, from a high of more than 60% at the eastern end of the Uintas, to 0% at the western end. Given that individual summit flats can be diminished through lateral erosion by surrounding valley glaciers, and that the summit flats themselves were apparently never glaciated, this result suggests that glacial erosion has been more effective in the western Uintas over the course of the Quaternary. Focused glacial erosion at the upwind end of the range is consistent with the hypothesis that the proximity of Lake Bonneville enhanced precipitation over the western Uintas during the Last Glacial Maximum [Munroe, J.S., and, Mickelson, D.M., 2002. Last Glacial Maximum equilibrium-line altitudes and paleoclimate, northern Uinta Mountains, Utah, U.S.A. Journal of Glaciology, 48, 257–266].


*Keywords:* Uinta Mountains; Summit flats; Erosion surfaces; Periglacial; Quaternary

## 1. Introduction

Isolated, laterally extensive, gently sloping surfaces are present at high elevations in many Laramide ranges of the western U.S. These "summit flats" (sensu Small and Anderson, 1998), prominent components of alpine landscapes, have been targets of investigation and speculation for more than a century (see Scott, 1975; Bradley, 1987). Much of this attention has been focused on the genesis of summit flats, specifically on whether summit flats are remnants of extensive erosion surfaces formed before mountain uplift (Mears, 1993; Scott, 1975) or if they developed in situ through intense periglacial weathering (Mackin, 1947), perhaps as cryoplanation terraces (Nelson, 1989, 1998). Despite decades of attention, however, difficulties with dating and semantic confusion continued to obscure understanding of these unique landforms into the late 20th century (Bradley, 1987).

Recent work on feedbacks between erosion, isostatic uplift, and glaciation (e.g. Brozovic et al., 1997; Montgomery and Greenberg, 2000; Small and Anderson, 1995) has reenergized research on summit flats because

*E-mail address:* jmunroe@middlebury.edu.

0169-555X/$ - see front matter © 2005 Elsevier B.V. All rights reserved.
doi:10.1016/j.geomorph.2005.07.030

of the utility of summit flats as geomorphic markers for constraining rates of valley incision and evolution of alpine landscapes. Furthermore, the development of cosmogenic surface exposure dating has given geomorphologists a powerful tool for quantifying rates of processes germane to the development of summit flats. For example, Small et al. (1997) used cosmogenic nuclides to document long-term rates of erosion of bedrock surfaces on summit flats in the Beartooth Range, Wind River Range, Front Range, and Sierra Nevada. Later, Small and Anderson (1998) investigated the development of geophysical relief through landscape erosion in the Beartooth Range, Wind River Range, Front Range and the Uinta Mountains. Most recently, Small et al. (1999) and Anderson (2002) worked in the Wind River Range, focusing on rates of regolith production and overall evolution of summit flats, respectively. Collectively, these studies support the theory that summit flats formed in situ under the influence of a periglacial climate during the late Cenozoic (Anderson, 2002).

Despite this resurgent interest in summit flats and their suitability as geomorphic markers, questions remain about the genesis of summit flats. For instance, Anderson (2002) notes that the roles of solifluction and chemical denudation in the formation of summit flats have not been rigorously addressed. Similarly, although Small and Anderson (1998) considered the distribution of summit flats in their investigation of the production of Laramide relief, the detailed pattern and form of summit flats within a single range have not been specifically investigated. This omission is notable because the intra-range arrangement of summit flats could provide additional information about the processes responsible for their development, especially if their distribution and morphometry were compared with known climatic, tectonic, or erosional gradients.

I examined summit flats in the Uinta Mountains, a Laramide range where these features are particularly well developed, and one of the ranges in which Small and Anderson (1998) investigated the production of relief. I sought answers to two main questions: First, how does the distribution of summit flats vary within an individual Laramide Range? And second, how does this distribution compare with gradients of precipitation and Pleistocene glaciation identified by previous work (Munroe, 2001; Munroe and Mickelson, 2002)? Accordingly, the main objectives of my study were 1) to document the spatial distribution and morphometry of summit flats in the Uintas, 2) to quantify their abundance as a percentage of total high-altitude area in different sections of the range, and 3) to examine possible climatic controls on their distribution. In this paper I first introduce the summit flats of the Uintas and provide a brief overview of prior research on them. Next, I describe the distribution and morphometry of summit flats within the range. Finally, I discuss this pattern and present a possible link between the distribution of summit flats, intensity of glacial erosion, and patterns of orographic precipitation during Pleistocene glaciations.

## 2. Summit flats of the Uinta Mountains

### *2.1. The Uinta Mountains*

The Uinta Mountains extend for ~200 km west to east across northeastern Utah and into northwestern Colorado. This study focuses on the higher western Uintas, which are not currently glacierized, but were extensively glaciated during the late Pleistocene (Fig. 1). On the basis of recently updated geomorphic mapping, glaciers covered approximately 1000 km$^2$ of the north side of the range (Atwood, 1909; Munroe, 2001), and nearly 1500 km$^2$ of the south side (Atwood, 1909; Laabs, 2004) during the Last Glacial Maximum (LGM). The core of the Uintas consists of the Uinta Mountain Group, a thick sequence of upper Precambrian siliciclastic rocks and lightly metamorphosed quartzite, which has been folded into an extensive, doubly plunging, anticline with an axis concordant with the central mountain ridgecrest (Hansen, 1969). The west–east orientation of the Uintas is unique among the Laramide ranges, and makes the Uintas an ideal location in which to investigate geomorphic gradients in a direction parallel to prevailing storm tracks and precipitations trends (Munroe and Mickelson, 2002).

### *2.2. The bollies*

Summits flats are particularly well developed and accessible at the eastern end of the glaciated Uintas where they are known locally as “bollies”. These landforms are uniformly gently sloping with convex-upward surface profiles (Fig. 2). Bedrock outcrops are rare, and no evidence of fluvial activity beyond local slopewash is present. Tors are uncommon. Erratics and striated clasts are completely absent, suggesting that the bollies were never glaciated. Overall, the bollies in the Uintas match the detailed descriptions of summit flats in the Wind River Range given by previous studies (Small et al., 1997; Small et al., 1999; Anderson, 2002).

The bollies are commonly mantled by regolith containing grain sizes from silt through coarse boulders (Bradley, 1936). Olson (1962) reported that most soils

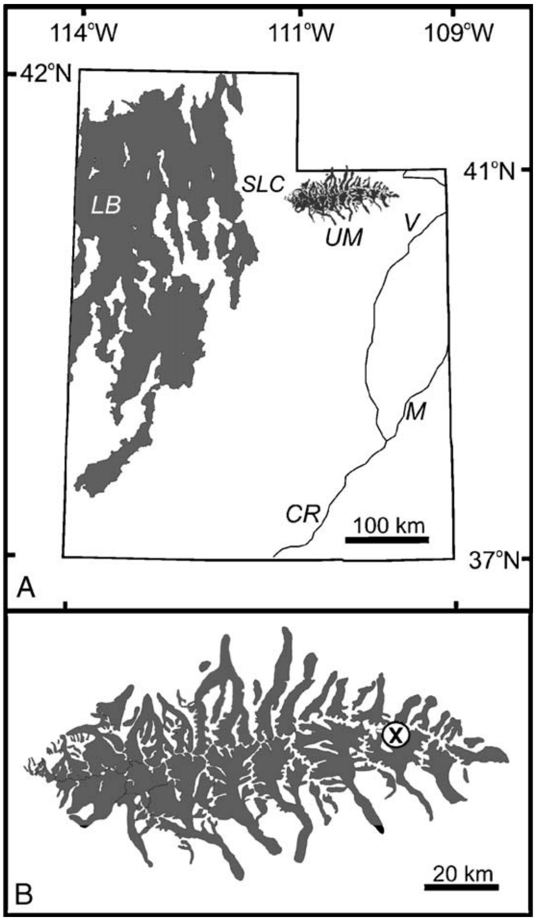


Fig. 1. (A) Map showing the outlines of Last Glacial Maximum (LGM) glaciers in the Uinta Mountains (UM) of northeastern Utah (Munroe, 2001; Munroe and Mickelson, 2002; Shakun, 2003), and the approximate outline of Lake Bonneville (LB, from the Utah Automated Geographic Reference Center, http://agrc.its.state.ut.us/) at the LGM. SLC = Salt Lake City; V = Vernal; M = Moab; CR = Colorado River. (B) Enlargement showing the outlines of the LGM glaciers in the Uintas. X marks the locations of the Chepeta RAWS and SNOTEL stations.

on the bollies contained >50% boulders by volume. The thickness of this regolith is unknown, however, it is likely >1 m as bedrock was not encountered in the few soil pits excavated on these landforms (Olson, 1962). In places this regolith forms a smooth mantle, carpeted by tundra vegetation (Bradley, 1936). In other areas, stony regolith has been reworked into well-developed periglacial features (Munroe, 2001) including sorted polygons up to 10 m in diameter (Fig. 2), and sorted stripes up to 3 m wide. Stones comprising polygon rims are lichen-covered, and turf cover is continuous in polygon centers, suggesting that these features are currently inactive. Numerous less organized features, including frost boils (van Everdingen, 2002), are also common on the bollies. The centers of most frost boils expose mineral soil devoid of larger clasts, indicating that these features are actively cryoturbating (Olson, 1962).

### 2.3. Climate

A Remote Automated Weather Station (RAWS) on the ridgeline in the eastern Uintas provides direct measurements of meteorological conditions on the bollies. The RAWS is located ~5 km west of Chepeta Lake (USGS Chepeta Lake quadrangle) at an elevation of 3705 m (Fig. 1), and is the highest RAWS in the United States. Data captured by the RAWS (WRCC, 2004) indicate that the mean annual temperature from January 1999 through December 2003 was −2.0 °C (Fig. 3). The mean annual wind speed is 6.2 m $s^{-1}$. Air temperatures during the summer (June/July/August) average 8.2 °C, while winter temperatures (December, January, February) average −10.2 °C. Air temperatures fluctuate above and below 0 °C frequently during the spring and fall. In 1999 the RAWS recorded 87 freeze–thaw cycles, although the actual number was likely greater because the RAWS records only average hourly temperatures, and because ~2% of the temperature data are missing from the 1999 record.

Snow is not accurately recorded by the unheated RAWS, but frozen precipitation is measured at an automated Snowpack Telemetry (SNOTEL) station located 2.5 km southeast of Chepeta Lake at an elevation of 3150 m (Fig. 1). Total annual precipitation at the Chepeta SNOTEL has averaged 80 cm $year^{-1}$ since 1990, with 48% of that accumulating as snow. Mean monthly precipitation ranges from 4 to over 8 cm, reaching maximum values in March and September, with annual minima in June and December (Fig. 3). Taken together, data from the Chepeta RAWS and SNOTEL indicate that summit flats in the Uinta Mountains experience a strong periglacial climate with abundant water for cryogenic weathering.

### 2.4. Historical overview

Bradley (1936) provided the most detailed study of summit flats in the Uintas. On the basis of concordance in elevation and slope, he concluded that the isolated flats were remnants of an extensive peneplain-like feature that he named the Gilbert Peak erosion surface. Because of the lack of evidence for extensive weathering and the abrupt slopes of local residual hills, Bradley concluded that the Gilbert Peak erosion surface formed not as a classic peneplain, but as a pediment during a

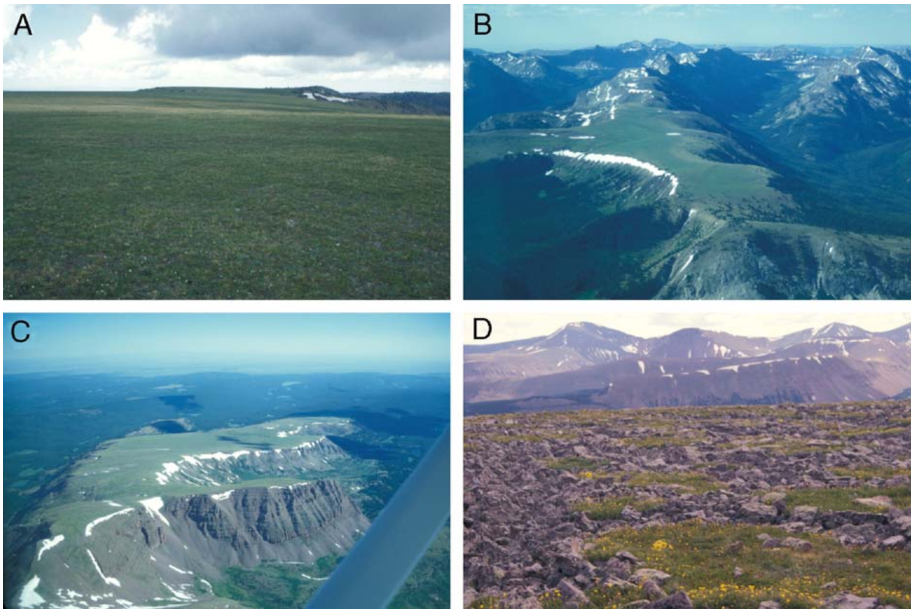


Fig. 2. (A) Landscape view of a summit flat surface. (B) Aerial view (looking southward) of a summit flat showing evidence of lateral erosion by cirque and valley glaciers. (C) Oblique aerial view of a typical summit flat in the Uinta Mountains (looking northward). (D) Sorted stone polygons on a high-elevation summit flat (3800 m) in the central Uinta Mountains.

long period of erosion and deposition under a semiarid climate (Bradley, 1936).

Bradley (1936) identified remnants of the Gilbert Peak surface at elevations from over 4000 m to 2200 m, and in positions up to 20 km from the ridgecrest. His Gilbert Peak erosion surface is, therefore, significantly more extensive than the summit flats considered in this study. This study does not attempt to evaluate the concept of the Gilbert Peak erosion surface. Instead summit flats in the Uintas are considered products of long-term weathering and erosion during which a pre-existing landscape, of unknown form, evolves to a predictable pattern of deep glacial valleys separated by interfluves having a summit flat morphology (Anderson, 2002). Thus, while the lower surfaces studied by Bradley (1936) may indeed be remnants of an ancient landscape created before incision of the modern glacial valleys, this analysis considers the current form of the higher summit flats a result of the dominant periglacial weathering regime active over the late Cenozoic.

## 3. Methods

In pursuit of the objectives outlined above, summit flats were identified in a GIS using elevation data collected by the Shuttle Radar Topography Mission (SRTM). The SRTM data were queried using maximum slope and minimum elevation criteria to produce a map of summit flats in the Uintas, allowing qualitative study of the pattern of summit flats throughout the range. This pattern was then addressed quantitatively by partitioning the Uintas into 10-km-wide swaths, and normalizing the area of summit flats in each swath to the total unglaciated area above an elevation threshold. Finally, the resulting trend in the area of summit flats along the range was compared with gradients of latest Pleistocene precipitation (Munroe and Mickelson, 2002) to elucidate possible controls on the distribution of summit flats.

### 3.1. Identification of summit flats

SRTM data covering the Uinta Mountains area were downloaded from the USGS Seamless Data Distribution System (USGS, 2004). The SRTM data have a nominal pixel resolution of 30 m, and lack the artificial boundaries often prominent in digital elevation models (DEMs) made by concatenating individual 7.5-min data sets. As such, the SRTM data are particularly well suited for analyses at the range scale. SRTM data covering the Uinta Mountains region were imported into a GIS in band-interleaved-by-line format. This file included pixels classified as “no data” in areas of extremely steep topography (for instance cirque headwalls). The number of “no data” pixels in the study area, however, is ~0.2% of the total, so the missing values were inconsequential in subsequent calculations.

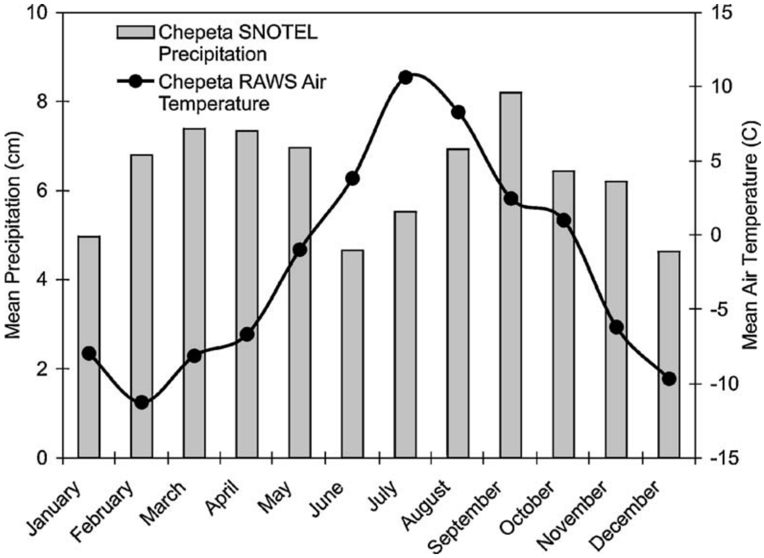


Fig. 3. Mean climatic data at the Chepeta SNOTEL station (precipitation, 3150 m) and the Chepeta RAWS (temperature, 3705 m) illustrating the strong periglacial climate of the Uinta summit flats.

The SRTM data were converted to raster format, producing a DEM of the Uinta Mountains. A second raster was then generated from this DEM by highlighting pixels with pixel–pixel slopes of $<0.3$ m $m^{-1}$ and an elevation of $>3400$ m. The maximum slope was selected to match the methodology of Small and Anderson (1998), and was confirmed by field observations in the Uintas. The minimum elevation threshold of 3400 m was selected to identify only those surfaces above the elevation of pervasive glacial erosion, as approximated by the elevations of cirque floors and reconstructed glacier equilibrium lines for the LGM (Munroe and Mickelson, 2002; Shakun, 2003). Field observations reveal that surfaces below this elevation depart from the classic summit flat form in that they generally lack periglacial features, are more impacted by fluvial processes, and are mantled by thicker regolith. The resulting data set was cleaned by removing the few high elevation cirque floors and lakes that met the elevation and slope criteria, and by deleting individual summit flat polygons with areas $<5\times10^{-2}$ $km^2$. This threshold was arbitrarily chosen to eliminate polygons that met the summit flat criteria mathematically but not geomorphically. The final product of this process was a map delineating the summit flats of the Uinta Mountains. This map was used to clip the original DEM to allow quantification of the elevation range and slopes of individual summit flats. This procedure was then repeated using a minimum elevation of 3000 m to evaluate the sensitivity of this analysis to the elevation threshold selected.

### *3.2. Determination of range-wide variation*

The area of summit flats in different sections of the Uintas was documented in twelve non-overlapping, 10-km-wide, north- to south-orientated swaths. These swaths were used to clip the map of summit flats, allowing calculation of the total area of summit flats in each swath. Next, the swaths were used to clip the original DEM, and the total land area above 3400 m and outside the margins of reconstructed late Pleistocene glaciers in each swath was calculated. The two values were then used to compute the percent of non-glaciated land above 3400 m having a summit flat morphology in each swath. Resulting areas and percent values were plotted against the UTM easting of the central meridian of each swath to reveal the variation in summit flat area with position in the range.

## 4. Results

Summit flats cover 193.42 $km^2$ in the Uinta Mountains, 43% of the unglaciated landscape above 3400 m (Fig. 4). Local pixel-scale slopes on the summit flats range from 0° to the upper threshold of 16.7° with a mean of 8.9°. Individual summit flat segments range in area from the lower threshold of $5\times10^{-2}$ $km^2$, to 33.77 $km^2$, with a mean of 1.21 $km^2$. The largest continuous summit flats, the extensive bollies, are located at the eastern end of the range. Despite the operation to remove summit flats with areas $<5\times10^{-2}$ $km^2$, small summit flat segments are considerably more common

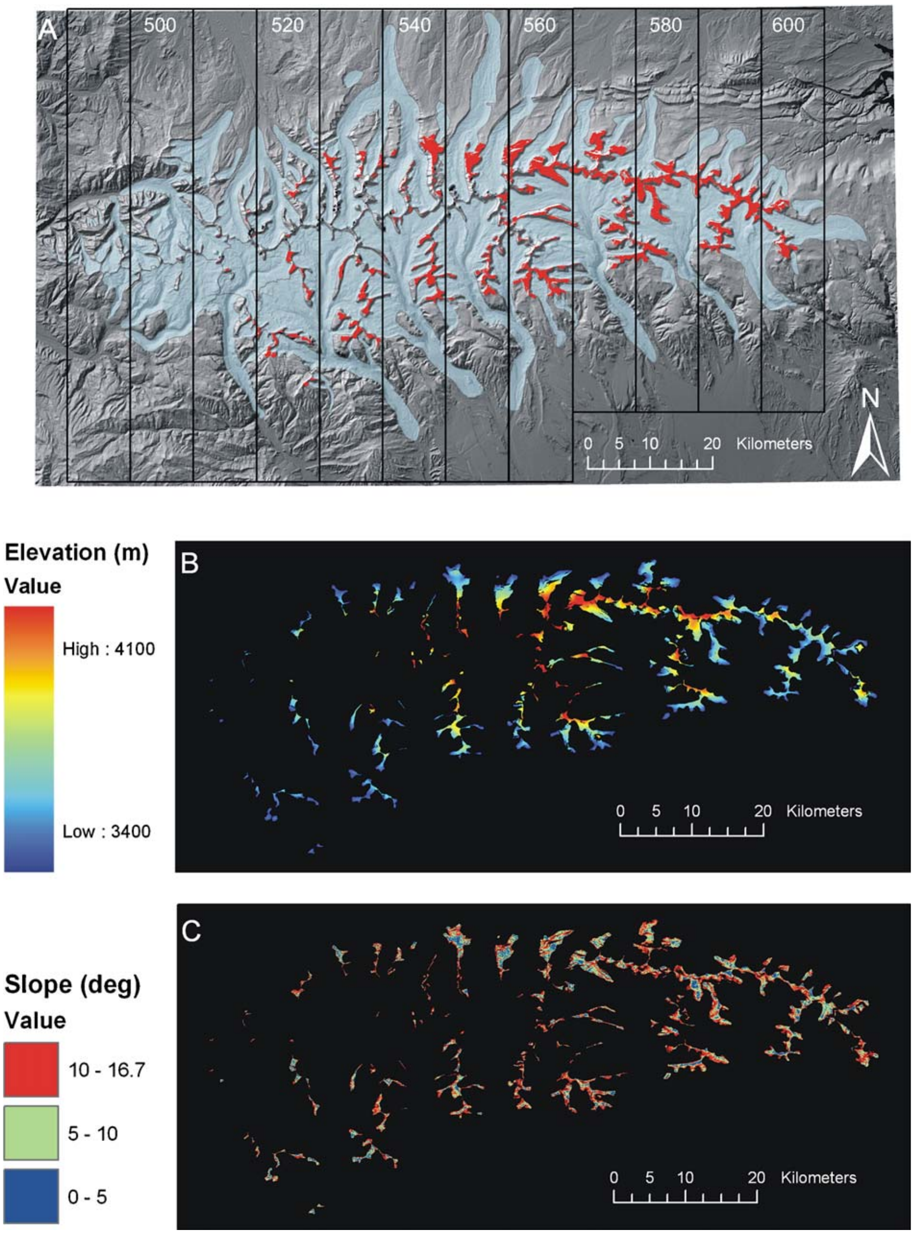


Fig. 4. (A) Distribution of summit flats in the Uinta Mountains (red) and outlines of LGM glaciers (light blue) displayed over a 30-m digital elevation model. A dramatic decrease in total summit flat area occurs at the west end of the range. The 10-km-wide swaths used in calculating percent summit flats are also shown with the UTM easting in km (see text). (B) Elevations of summit flats. Flats reach their maximum elevations along the ridgecrest and near the range center. Flats at the eastern end of the Uintas are present on the ridgecrest, while those at the western end are limited to interfluves because the ridgecrest has been reduced to a series of arêtes and horns. (C) Slopes of summit flats. Note the generally convex surfaces of the larger summit flats and the gentle gradients.

than large segments, as illustrated in Fig. 5, and as quantified by the large positive skewness (7.3) for the distribution of summit flat areas. This situation is partially an artifact of the identification process for summit flats that excluded locally steep areas, leading to segmentation of larger, essentially continuous, summit flats. Nonetheless, the trend of increasing rarity of larger summit flats is realistic given the overall altitude-area distribution in the Uintas (Fig. 6), which displays a nearly monotonic decrease of area at elevations above ~3000 m.

The distribution of high-elevation land and summit flats varies throughout the Uintas. The total land area above 3400 m increases towards the center of the range,

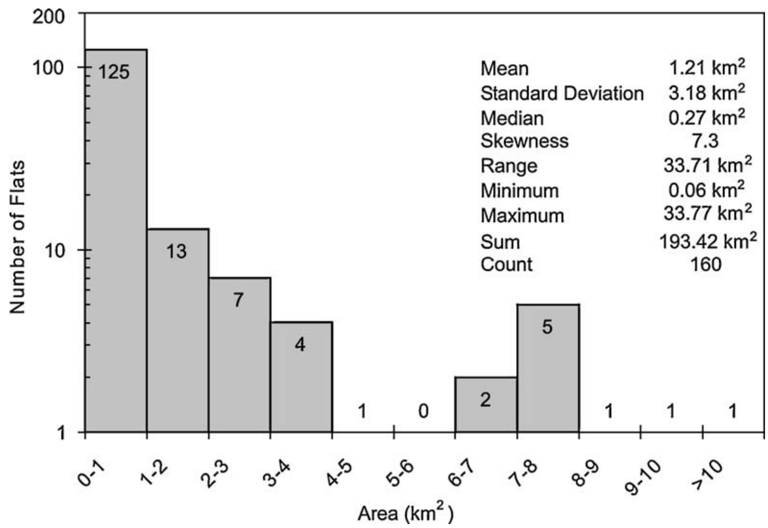


Fig. 5. Frequency distribution of summit flat areas in the Uinta Mountains. Only surfaces greater than $5 \times 10^{-2}$ km$^2$ were considered in this analysis (see text).

reflecting the structure of the doubly plunging anticline that defines the Uinta Mountains. Less than 40 km$^2$ rises above 3400 m in each 10-km-wide swath at the eastern end of the range, and no parts of the landscape rise above this elevation at the western end. In contrast, near the range center, up to 80 km$^2$ are above 3400 m in each swath (Fig. 7A). The area of summit flats follows a somewhat similar trend, with the smallest areas per swath found at the extreme eastern (9 km$^2$) and western (0 km$^2$) ends of the range, with higher values (up to 37 km$^2$) in the center (Fig. 7A). Yet overall, the area covered by summit flats decreases from east to west (see Fig. 4). This impression is supported by the normalized area data, which reveal that more than half (up to 69%) of the area above 3400 m in the eastern 30 km of the Uintas meets the definition of summit flats (Fig. 7A). Moving west along the ridgecrest, however, the percent of summit flats decreases to 40–50% near the range center, and then falls to 0% at the western end. The overall rate of decrease averages 0.6% km$^{-1}$.

Comparable results were obtained using 3000 m as a lower threshold for the identification of summit flats (Fig. 7B). Selection of this value greatly increases the area of summit flats (958.40 km$^2$) and slightly increases

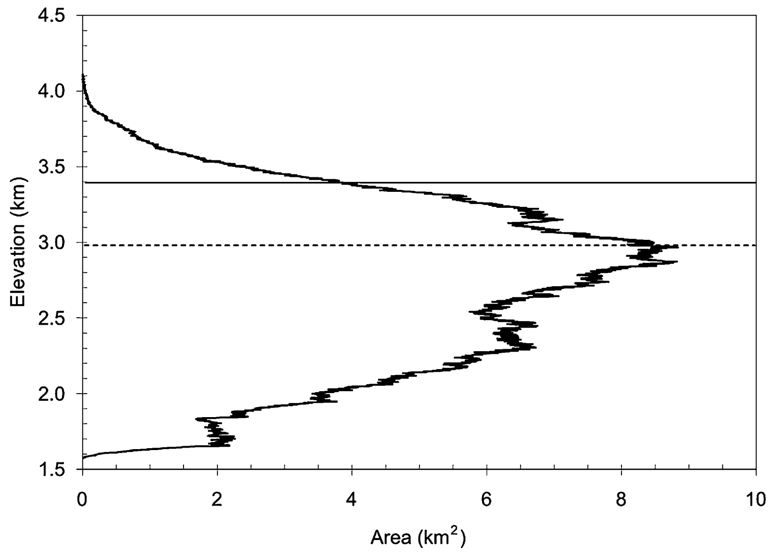


Fig. 6. Hypsometry of the Uinta Mountains. Elevations range from 1576 m (arbitrary boundary of study area) to 4115 m, with a mean of 2700 m. The 3400- and 3000-m thresholds used in delineating summit flats are highlighted.

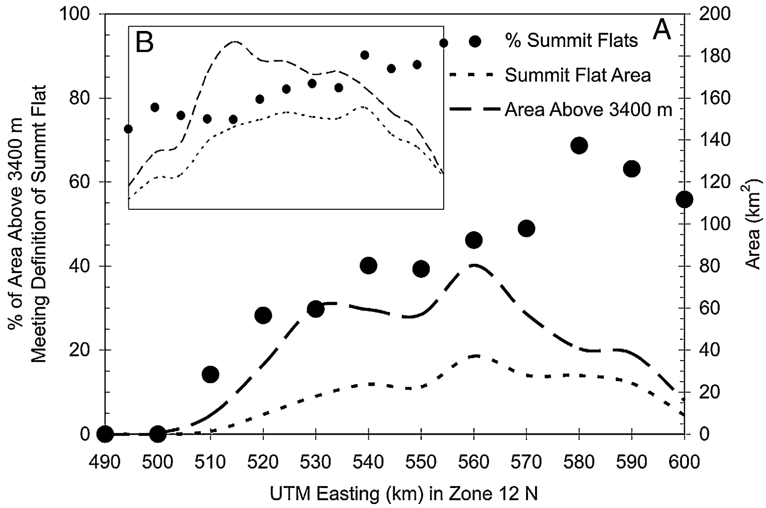


Fig. 7. (A) Unglaciated area above 3400 m, summit flat area, and percent summit flats in the Uinta Mountains. (B) Results from identical analysis using 3000 m as the lower elevation for delineating summit flats (axes ranges are the same). Both data sets show a pronounced decrease in the percentage of high altitude area occupied by summit flats in the western Uintas.

their overall abundance (66%). When considered as a percentage of unglaciated land above 3000 m, however, a similar pattern emerges, with values reaching 90% at the eastern end, fluctuating around 60–70% near the range center, and dropping below 50% at the western end. Thus, the overall trend toward decreasing abundance of summit flats in the western Uintas is insensitive to the selection of 3000 m or 3400 m as a lower elevation threshold.

## 5. Discussion

### *5.1. Summit flat distribution*

Summit flats are major components of the alpine landscape in the glaciated Uinta Mountains. At the eastern end of the range, the classic bollies form extensive, gently sloping surfaces on interfluves and the main ridgecrest. The modest slopes of these uplands are accentuated by the gently dipping structure of the Uinta Mountain anticline near the fold axis, producing strongly developed "biscuit-board" topography (see Fig. 2). Bradley (1936) incorporated this landscape into his argument, stating "Locally, however, smooth portions of the Gilbert Peak surface cross the range and slope southward, being the headward remnants of that surface which once flanked the south side of the range… Indeed, the whole crest line of the Uinta Range from South Burro Peak for many miles eastward is a well-preserved portion of this ancient topography" (Bradley, 1936 p. 171). In contrast, in the western Uintas, the ridgecrest narrows to a winding arête, and summit flats are less extensive and present mainly on interfluves. The significance of this change is unclear, but it appears related to the greater degree of topographic inundation of the western Uintas by LGM glaciers.

### *5.2. Insights into long-term processes*

The development of dating methods using cosmogenic radionuclides has allowed quantification of their processes responsible for the development of summit flats, improving of understanding of their genesis. Given the difference between rates of bedrock weathering ($6.9 \pm 2.8$ m $Ma^{-1}$) and regolith production ($14.3 \pm 4.0$ m $Ma^{-1}$) determined from $^{10}Be$ concentrations, Small et al. (1999) concluded that summit flats in the Wind River Range began forming contemporaneously with the onset of glaciation in the latest Pliocene (2–3 Ma). More recently, Anderson (2002) modeled the evolution of summit flats given the order-of-magnitude disparity between rates of periglacial erosion on summit flats and mean rates of glacial erosion into crystalline rock (Small and Anderson, 1998). He concluded that incision of glacial valleys greatly exceeds the rate of lowering of the summit flats, a situation that decoupled the flats from erosion in the glacial valleys soon after the onset of glaciation (Anderson, 2002). The convex-upward profile common to summit flats is, therefore, an equilibrium condition, and summit flats are a predictable product of slow weathering and periglacial hillslope processes (Anderson, 2002).

If summits flats form in situ through the evolution of interfluves stranded between deepening glacial valleys, then the decrease in proportion of the landscape dominated by summit flats in the western Uintas implies slowing of the processes responsible for formation, or acceleration of the processes responsible for destruction. There is no reason to believe that the periglacial processes Anderson (2002) considered responsible for the formation of summit flats (frost creep and regolith formation driven by frost frequency) differ at the western end of the Uintas. Thus, the explanation for the non-uniform distribution of summit flats may lie with processes that eliminate summit flats over time. Anderson (2002) demonstrated that summit flats are effectively isolated from the erosive processes that result in deepening of glacial valley, but glaciers can also erode laterally. For small glacier systems, the conversion of V-shaped fluvial valleys to U-shaped glacial valleys can be accomplished without valley widening (Harbor, 1992; Hirano and Aniya, 1988). With larger drainage areas, however, glacial valleys become progressively wider than fluvial valleys, indicating that larger glaciers can effectively broaden valleys at the expense of interfluves (Montgomery, 2002). Similar results were reported from a comparison of fluvial and glacial valleys in the Uintas (Carson, 2004). Valley widening through glacial erosion reduces summit flat dimensions, but has no direct effect on the surface form of the interfluves themselves (Anderson, 2002). Thus, we can consider the spatial dimensions of a given summit flat to reflect the efficacy of cliff backwearing through glacial erosion.

Additional evidence that Pleistocene glacial erosion was more extensive in the western Uintas is provided by a consideration of the volume of the valleys. If it can be assumed that the modern form of the Uinta valleys results primarily from glacial erosion, then valley volume can be used as a proxy for erosional efficacy given the overall uniformity of rocks in the Uinta Mountain Group. To generate these data, I fit a spline surface to the summit flat map described in Section 3.1, and subtracted the modern topography to quantify the amount of material removed from the landscape to form the glacial valleys. I then partitioned this new data set with non-overlapping 10-km swaths (see Section 3.2) to explore the relationship between erosion and position along the west–east extent of the Uintas. The amount of surface lowering in swaths at the eastern end of the range averages 150 m pixel$^{-1}$, but rises steadily to >350 m pixel$^{-1}$ at the western end (Fig. 8). Thus, it appears that glaciers in the western Uintas were more effective at eroding the pre-Quaternary landscape.

### 5.3. Assumptions

It follows from this logic that the decrease in percent summit flats at the western end of the Uintas is a manifestation of more intense glacial erosion there over the course of the Quaternary. Several important assumptions are implicit in this statement, most notably that the original density of fluvial drainage exploited by Pleistocene glaciers was uniform along the range, and that lithologic differences between the eastern and western ends of the Uintas that might control rock resistance are minimal. These assumptions can be justified, however, by considering several characteristics of the modern distribution of major rivers in the Uintas, and the overall structure of the Uinta anticline. First, because the ridgecrest is nearly concordant with the fold axis,

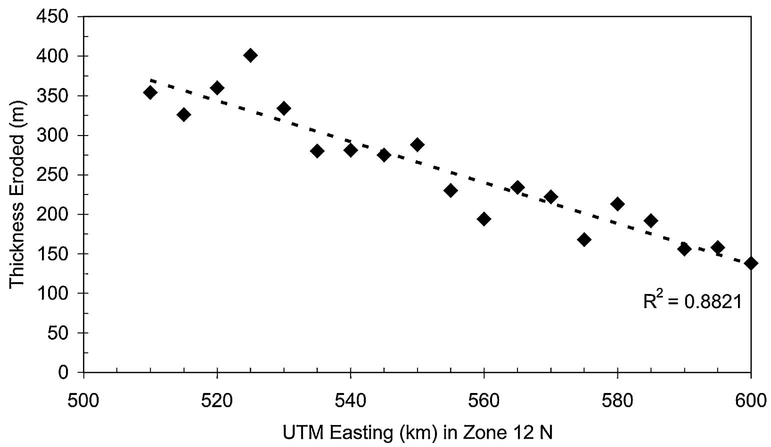


Fig. 8. Average erosion in the Uintas (in m pixel$^{-1}$) calculated from the difference between the modern surface topography and a spline surface fit to the summit flats shown in Fig. 4. Glacial valleys in the western Uintas are eroded considerably deeper than those in the eastern Uintas, suggesting that western glaciers were more effective agents of erosion during the Quaternary.

the overall bedrock dip parallels the surface slope and varies little from one end of the range to the other. Second, major rivers are fairly evenly spaced across the north and south slopes, suggesting that the pre-glacial drainage density was uniform. Third, while drainages do become increasingly complex from east to west across the northern Uintas, this trend reflects greater integration of tributaries in the western valleys and does not necessarily require a more complicated initial drainage pattern in this area. Fourth, although Atwood (1909) remarked on greater width of south slope headwater basins compared with those on the north side, all major south slope rivers head in expansive valleys, likely reflecting the more gentle dip of rock units on the south limb of the asymmetric anticline. Finally, while the Uinta Mountain Group bedrock is a complicated assortment of clastic sedimentary rocks at fine scales, at the range scale the rocks are fairly uniform. This assertion is supported by the lack of an obvious trend in the efficacy of post-glacial fluvial etching in the glacial troughs: although some of the larger rivers, especially on the south slope, currently flow in bedrock canyons several tens of meters deep, no trend exists in the distribution of these features along the range, suggesting that the rocks are equally resistant to erosion (Atwood, 1909).

### 5.4. Explanation

The obvious question is why were Pleistocene glaciers more effective at eroding the western Uintas? The answer may lie with the distribution of precipitation in the range. Prevailing west-to-east winds at the latitude of the Uintas preferentially deliver orographic precipitation to west-facing slopes. The modern snow-water-equivalent gradient on the western slope of the Wasatch Range, immediately west of the Uintas, is the steepest in the Great Basin (1.37 m km$^{-1}$), indicating the efficiency with which this range intercepts westerly derived moisture (Zielinski and McCoy, 1987). Because orographic precipitation depletes the moisture content of winter storms as they sweep across progressively higher mountains (Houghton, 1979), the western summits of the Uintas should receive increased snowfall at the expense of the eastern end of the range. This effect is demonstrated by the distribution of annual maximum SWE readings at SNOTEL sites, which reach a maximum in the western Uintas (Munroe and Mickelson, 2002). Zielinski and McCoy (1987) concluded that late Pleistocene circulation patterns across the northern Great Basin were similar to those of today, and climate simulations suggest that the jet stream and storm tracks were displaced southward by the Laurentide Ice Sheet, reinforcing a dominantly westerly airflow through this region (COHMAP, 1988). Orographic precipitation, therefore, may have produced larger glaciers with greater ice flux in the western Uintas, leading to more intense glacier erosion, (Hallet et al., 1996; Harbor, 1992; MacGregor et al., 2000) which reduced the area of summit flats relative to parts of the range farther east.

If orographic precipitation exerts a control over intra-range distribution of summit flats, then flats should be less common on the western slopes of all Laramide ranges predominantly influenced by west-to-east circulation. In their report on geophysical relief production in the Laramide ranges, Small and Anderson (1998) provide a map of summit flats in the northern Wind River Range (their Fig. 2b). I replicated this map using SRTM data for the Wind River Range, applying their upper slope threshold (0.3 m m$^{-1}$), a minimum elevation of 3000 m, and the methodology presented in Section 3.2. Summit flats occupy 25% of the area above 3000 m in the eastern third of their study area, and decrease to ~10% on the west side of the range. Although the area of summit flats decreases in an upwind direction, this decrease is considerably less pronounced than in the Uintas. Thus, another agent in addition to conventional orographic precipitation must be responsible for the pattern observed in the Uintas.

### 5.5. Uniqueness of the Uintas

While orographic precipitation may play a role in the distribution of summit flats throughout the Laramide ranges, the Uintas present a singular situation for two reasons. First, the west–east orientation provides an extensive area of sustained high elevation that runs nearly parallel to the prevailing atmospheric circulation. In contrast, the other Laramide ranges are oriented predominantly north to south producing a relatively minor west–east dimension. For instance, the west–east width of the Wind River Range is less than half the east–west length of the Uinta Mountains. Thus, the orientation of the Uintas produces a long stretch of mountains over which a precipitation gradient can influence geomorphology.

Second, the Uintas are unique because the Bonneville Basin, located ~100 km upwind from the western end of the range, was occupied by a large pluvial lake at least four times (Oviatt et al., 1999), and possibly more (Eardley et al., 1973) during the Quaternary Period. The most recent of these lakes, Lake Bonneville, covered ~51,700 km$^2$ shortly after the LGM (see Fig. 1), attaining an altitude of ~1550 m before catastrophically spilling into the Snake River drainage of southern Idaho (O'Connor, 1993). Numerical simulations of climate in the Bonneville Basin during the LGM suggest that open water was present over deeper parts of the lake in January (Hostetler et al., 1994). This moisture source, combined with the abrupt topography downwind, would have enhanced orographic precipitation above interglacial levels. Hostetler et al. (1994) concluded that 23% of precipitation near Lake Bonneville at 18 ka resulted from lake–atmosphere feedbacks. Similarly, an attempt to model valley glaciers in the western Wasatch Mountains concluded that lake-induced precipitation played an important role in the hydrologic balance of Lake Bonneville and local valley glaciers (McCoy and Williams, 1985).

Enhancement of precipitation downwind of Lake Bonneville also appears to have influenced glaciers in the Uintas during the LGM. Munroe and Mickelson (2002) documented that LGM equilibrium line altitudes (ELAs) drop ~700 m from the range center to the extreme west end. As glacier ELAs are climatically controlled, paleo-ELAs deduced from glacier reconstructions can be used as a paleoclimate proxy. Munroe and Mickelson (2002) argued that the profound drop in ELAs reflects the presence of a steep precipitation gradient along the Uintas during the LGM, with proportionally more precipitation falling at the western end of the range. Given that the closed topography of the Bonneville Basin would force the development of at least a small lake during any pluvial period, the western Uintas were likely impacted by lake-enhanced precipitation frequently during the Quaternary. This situation may be responsible for the decrease in the area of summit flats towards the western end of the range.

In summary, the dramatic decrease in percent summits flats at the western end of the Uintas may be explained by a combination of: a) the unique orientation of the range parallel to the direction of prevailing moisture transport, b) increased glacial erosion conditioned by orographic precipitation, and c) the proximity of pluvial lakes in the Bonneville Basin, a unique, but extensive, local moisture source. Future work, including modeling atmospheric circulation downwind of Lake Bonneville, and patterns of glacial erosion in the range, should be undertaken to evaluate the hypothesis that the efficacy of glacial erosion, influenced by precipitation, is responsible for the distribution of summit flats.

## 6. Summary

Summit flats are an important component of the alpine landscape in the Uinta Mountains. 43% of the unglaciated land area above 3400 m has a slope of $<0.3$ m m$^{-1}$ (excluding high elevation cirque floors, lakes, and other "non-summit flat" surfaces). Areas of individual summit flats range up to 33.77 km$^2$, with the largest of these forming the "bollies" of the eastern Uintas. Small summit flats ($<1.0$ km$^2$) are considerably more common than large segments, although this distribution is somewhat biased by the nature of the technique used in the delineation of summit flats.

The area of summit flats and the total area $>3400$ m are greatest near the range center and lowest at the eastern and western ends. While extensive summit flats comprise more than 50% of the unglaciated landscape over 3400 m at the eastern end of the Uintas, this percentage drops to zero at the western end. Similar trends are noted when the lower elevation of summit flats is taken to be 3000 m. Assuming the preglacial form of the Uintas was a gently sloping upland (as suggested by the bedrock structure and the geomorphology of the summit flats themselves), and that the original distribution of preglacial valleys was uniform, this trend suggests that glacial erosion, which may be responsible for constraining the dimensions of summit flats through backwearing of headwalls and the cliffs of glacial troughs, has been more effective at the western end of the range over the course of the Quaternary. This interpretation is consistent with the theory that the western Uintas received orographic precipitation enhanced by the proximity of Lake Bonneville during the Last Glacial Maximum (Munroe and Mickelson, 2002). Furthermore, given that precursors to Lake Bonneville existed in at least three of the pre-LGM Quaternary glaciations (Oviatt et al., 1999), it is possible that the greater dissection of the western Uinta landscape is a result of glacial erosion enhanced by pluvial lake formation throughout the Quaternary.

The methodology reported here could be applied to other Laramide Ranges in which summit flats have been investigated. Although other ranges lack the unique west–east orientation of the Uintas, it would nonetheless be instructive to determine if trends in summit flat extent exist elsewhere, and to compare these trends with Pleistocene glaciation gradients (e.g. Meyer et al., 2004). Recently developed digital elevation data sets, along with the continued refinement of cosmogenic surface exposure dating, should move us closer to an improved understanding of these enigmatic landforms.

## Acknowledgments

My interest in the spectacular bollies of the Uinta Mountains was sparked by conversations with D. Koerner, and fieldwork with J. Bockheim and D. Douglass. E. Carson and B. Laabs provided valuable suggestions in the early stages of this study. T. Manley assisted with aspects of the GIS analysis. The clarity of the manuscript and thoroughness of the analysis benefited greatly from thoughtful reviews by R. Anderson and J. Harbor. Support was provided by NSF EAR-0345112.

## References


Anderson, R.S., 2002. Modeling the tor-dotted crests, bedrock edges, and parabolic profiles of high alpine surfaces of the Wind River Range, Wyoming. Geomorphology 46, 35–58.

Atwood, W.W., 1909. Glaciation of the Uinta and Wasatch Mountains. U.S. Geological Survey Professional Paper 61. 96 pp.

Bradley, W.H., 1936. Geomorphology of the north flank of the Uinta Mountains. U.S. Geological Survey Professional Paper 185-I, 163–199.

Bradley, W.C., 1987. Erosion surfaces of the Colorado Front Range: a review. In: Graf, W.L. (Ed.), Geomorphic Systems of North America. Centennial Special Volume. Geological Society of America, Boulder, CO.

Brozovic, N., Burbank, D.W., Meigs, A.J., 1997. Climatic limits on landscape development in the northwestern Himalaya. Science 276, 571–574.

Carson, E.C., 2004. Relative efficacy of glacial versus fluvial erosion in the Uinta Mountains, northeastern Utah. Geological Society of America Annual Meeting. Geological Society of America, Denver, CO p. 530.

COHMAP, 1988. Climate changes of the last 18,000 years: observations and model simulations. Science 241, 1043–1052.

Eardley, A.J., et al., 1973. Lake cycles in the Bonneville Basin, Utah. Geological Society of America Bulletin 84, 211–216.

Hallet, B., Hunter, L., Bogen, J., 1996. Rates of erosion and sediment evacuation by glaciers: a review of field data and their implications. Global and Planetary Change 12, 213–235.

Hansen, W.R., 1969. The geologic story of the Uinta Mountains. U.S. Geological Survey Bulletin 1291. 144 pp.

Harbor, J.M., 1992. Numerical modeling of the development of U-shaped valleys by glacial erosion. Geological Society of America Bulletin 104, 1364–1375.

Hirano, M., Aniya, M., 1988. A rational explanation of cross-profile morphology for glacial valleys and of glacial valley development. Earth Surface Processes and Landforms 13, 707–716.

Hostetler, S.W., Giorgi, F., Bates, G.T., Bartlein, P.J., 1994. Lake–atmosphere feedbacks associated with paleolakes Bonneville and Lahontan. Science 263, 665–669.

Houghton, J.G., 1979. A model for orographic precipitation in the north–central Great Basin. Monthly Weather Review 107, 1462–1475.

Laabs, B.J.C., 2004. Late Quaternary glacial and paleoclimate history of the southern Uinta Mountains, Utah. Ph.D. Thesis, University of Wisconsin, Madison. 162 pp.

MacGregor, K.R., Anderson, R.S., Anderson, S.P., Waddington, E.D., 2000. Numerical simulations of glacial-valley longitudinal profiles. Geology 28, 1031–1034.

Mackin, J.H., 1947. Altitude and local relief of the Bighorn area during the Cenozoic. 2nd Annual Field Conference. Wyoming Geological Association, pp. 103–120.

McCoy, W.D., Williams, L.D., 1985. Application of an energy-balance model to the late Pleistocene Little Cottonwood Canyon glacier with implications regarding the paleohydrology of Lake Bonneville. In: Diaz, H.F. (Ed.), Problems of and prospects for predicting Great Salt Lake levels. Center for Public Affairs and Administration, University of Utah, Salt Lake City, UT, pp. 40–53.

Mears, B.J., 1993. Geomorphic history of Wyoming and high-level erosion surfaces. In: Roberts, S.M. (Ed.), Geology of Wyoming. Memoir. Geological Survey of Wyoming, pp. 608–626.

Meyer, G.A., Fawcett, P.J., Locke, W.W., 2004. Late-Pleistocene equilibrium-line altitudes, atmospheric circulation, and timing of mountain glacier advances in the interior northwestern United States. In: Wood, S.H. (Ed.), Geological Field Trips in Southern Idaho, Eastern Oregon, and Northern Nevada, U.S. Geological Survey Open File Report 2004-1222, pp. 61–68.

Montgomery, D.R., 2002. Valley formation by fluvial and glacial erosion. Geology 30, 1047–1050.

Montgomery, D.R., Greenberg, H., 2000. Local relief and the height of Mount Olympus. Earth Surface Processes and Landforms 25, 386–396.

Munroe, J.S., 2001. Late Quaternary history of the northern Uinta Mountains, northeastern Utah. Ph.D. dissertation Thesis, University of Wisconsin-Madison, Madison, Wisconsin. 398 pp.

Munroe, J.S., Mickelson, D.M., 2002. Last Glacial Maximum equilibrium-line altitudes and paleoclimate, northern Uinta Mountains, Utah, U.S.A. Journal of Glaciology 48, 257–266.

Nelson, F.E., 1989. Cryoplanation terraces; periglacial cirque analogs. Geografiska Annaler. Series A: Physical Geography 71, 31–41.

Nelson, F.E., 1998. Cryoplanation terrace orientation in Alaska. Geografiska Annaler. Series A: Physical Geography 80, 135–151.

O'Connor, J.E., 1993. Hydrology, hydraulics, and geomorphology of the Bonneville Flood. Special Paper - Geological Society of America 274, 83.

Olson, O.C., 1962. Some soil–plant–erosion relationships on the Leidy Peak Uinta alpine area. US Forest Service Report, vol. 6200-7 (6/65), p. 24.

Oviatt, C.G., Thompson, R.S., Kaufman, D.S., Bright, J., Forester, R.M., 1999. Reinterpretation of the Burmester Core, Bonneville Basin, Utah. Quaternary Research 52, 180–184.

Scott, G.R., 1975. Cenozoic surfaces and deposits in the southern Rocky Mountains. In: Curtis, B.F. (Ed.), Cenozoic History of the Southern Rocky Mountains. Geological Society of America, Boulder, CO, pp. 227–248.

Shakun, J., 2003. Last glacial maximum equilibrium-line altitudes and paleoclimate, northeastern Utah. Geological Society of America Annual Meeting. Geological Society of America, Seattle, Washington, p. 541.

Small, E.E., Anderson, R.S., 1995. Geomorphically driven late Cenozoic rock uplift in the Sierra Nevada, California. Science 270, 277–280.

Small, E.E., Anderson, R.S., 1998. Pleistocene relief production in Laramide mountain ranges, western United States. Geology 26, 123–126.

Small, E.E., Anderson, R.S., Repka, J.L., Finkel, R., 1997. Erosion rates of alpine bedrock summit surfaces deduced from in situ $^{10}$Be and $^{26}$Al. Earth and Planetary Science Letters 150, 413–425.

Small, E.E., Anderson, R.S., Hancock, G.S., 1999. Estimates of the rate of regolith production using $^{10}$Be and $^{26}$Al from and alpine hillslope. Geomorphology 27, 131–150.

USGS, 2004. The National Map—Seamless Data Distribution System (http://seamless.usgs.gov) last accessed 4/30/05.

van Everdingen, R., 2002. Multi-Language Glossary of Permafrost and Related Ground-Ice Terms. National Snow and Ice Data Center/World Data Center for Glaciology, Boulder, CO.

WRCC, 2004. Western Regional Climate Center. http://www.wrcc.dri.edu, last accessed 4/30/05.

Zielinski, G.A., McCoy, W.D., 1987. Paleoclimatic implications of the relationship between modern snowpack and late Pleistocene equilibrium-line altitudes in the mountains of the Great Basin, western U.S.A. Arctic and Alpine Research 19, 127–134.